Phase transition for a $\frac{3}{8}$-monolayer Sn-adsorbed Cu(001) bimetallic surface alloy

Koichiro Yaji,* Ryuichi Nakayama, Kan Nakatsuji, Takushi Iimori, and Fumio Komori†
Institute for Solid State Physics, The University of Tokyo, Kashiwashi, Chiba 277-8581, Japan
(Received 14 October 2008; revised manuscript received 5 February 2009; published 31 March 2009)

Structural transition of 3/8 monolayer Sn-adsorbed Cu(001) surface alloy and the changes in the Sn-induced surface resonance band have been studied by low-energy electron diffraction and angle-resolved photoemission spectroscopy. The surface structure reversibly changes between $\begin{pmatrix} -4 & 2 \\ 0 & 4 \end{pmatrix}$ periodicity at low temperature and (1×1) periodicity at high temperature. This transition is interpreted as an *order-disorder* transition from the structure model while the resonance band of the 3/8-ML Sn/Cu(001) surface significantly changes with the transition. The band folds back with an energy gap with decreasing temperature through the transition temperature. The backfolding point of the band is close to the Fermi wave number in reciprocal space in the angle range between 0° and 11° from the $\bar{\Gamma}\bar{M}$ line, and is independent of surface Brillouin-zone boundary.

DOI: 10.1103/PhysRevB.79.115449 PACS number(s): 73.20.At, 68.35.Rh

I. INTRODUCTION

Origin of surface phase transition in low-dimensional materials is one of the most important topics because of their varieties and complexity. Typical examples are bimetallic surface alloys such as elements of groups 13 and 14 of the Periodic Table (In, Sn, Tl, and Pb) adsorbed on the Cu(001) in a submonolayer region. The surfaces have been both experimentally and theoretically studied for the structural transition and electronic states.[1–14] In these studies, the correlation was pointed out between the structural transition and formation of an energy gap in a surface resonance band around the Fermi energy (E_F).

Among these, tin-adsorbed Cu(001) surfaces [Sn/Cu(001)] have been studied for more than two decades because their morphologies largely depends on the tin coverage in submonolayer range. Four ordered structures of the Sn/Cu(001) surfaces were first systematically studied by Argile and Rhead.[15,16] The surface structures were reinterpreted by McLoughlin *et al.*[17] using a quantitative analysis of energy-dependent low-energy electron-diffraction intensity (LEED-*IV*), in which structural models for the three phases have been proposed. The phases had 1/5-monolayer (ML), 1/3-ML, and 1/2-ML of Sn, where ML is defined as the surface density of Cu atoms on the Cu(001)-1×1 surface. Thenceforth, the Sn/Cu(001) surfaces have been studied by several methods, such as scanning tunneling microscopy (STM), LEED, and surface x-ray diffraction (SXRD) for each phase.[8,18–22] These studies clarified that the surface structures of the 1/5-ML and 1/3-ML Sn/Cu(001) are stable below ~450 K.[20] Whereas, the surface of the 1/2-ML Sn/Cu(001) shows a temperature induced reversible phase transition as described above.[8,13,14]

Recently, a new phase has been reported between the 1/3-ML and 1/2-ML Sn/Cu(001) surfaces by means of LEED, SXRD, and STM.[20–22] J. M. Blanco *et al.*[20] showed in their LEED observation that the surface of the new phase has $\begin{pmatrix} -4 & 2 \\ 0 & 4 \end{pmatrix}$ periodicity at 300 K. They also claimed that the LEED pattern showed a $p(2 \times 2)$ structure at 440 K. Nara *et al.*[21] reported its atomic image at room temperature (RT) using STM and proposed a simple model of the Sn arrangement at the surface with Sn coverage of 3/8 ML.[21,22] However, the nature of the structural transition above RT has been unclear.

It is important that the origin of the structural transitions for the Sn/Cu(001) surface alloy systems is clarified. Concerning 1/2–ML Sn/Cu(001), the surface shows the structural transition at 360 K accompanied with a gap formation of the electronic states at surface Brillouin-zone (SBZ) edge.[8,13,14] Blanco *et al.* claimed that the transition is attributed to Peierls-type charge density wave (CDW).[8,13] The type of CDW strongly depends on the strength of electron-phonon coupling.[11] In the case of weak-coupling, CDW correlation length is much longer than the CDW period. On the other hand, strong-coupling CDW is characterized by a wide band gap and a short CDW correlation length. In Ref. 11, the CDW transition for In and Sn on Cu(001) surfaces was classified into a new category with a strong coupling and a long CDW correlation length. Recently, however, the authors' group has shown that the phase transition in 1/2-ML Sn/Cu(001) is inconsistent with the exiting views of CDW.[14]

In the present paper, we report the surface structure and electronic states of 3/8-ML Sn/Cu(001) surface, and discuss the origins of the structural transition and changes in electronic states. The surface atomic image has been taken by means of STM at RT. The modification of the surface periodicity has been investigated by LEED observations between 125 K and 425 K. The 3/8-ML Sn/Cu(001) surface shows the reversible phase transition, in which the $\begin{pmatrix} -4 & 2 \\ 0 & 4 \end{pmatrix}$ periodicity at the low-temperature (LT) phase becomes the (1×1) periodicity at the high-temperature (HT) phase. The observed periodicity at the HT phase in the present study is different from that reported previously.[20] Critical exponent for the structural transition has been explored by observing the temperature dependence of the LEED intensity. The valence electronic states were measured by an angle-resolved photoemission spectroscopy (ARPES). We focused on a tin-induced surface resonance band, which crosses the Fermi energy in the $\bar{\Gamma}\bar{\mathrm{M}}$ direction in the HT phase. This band has an energy gap in the LT phase as in the case of the 1/2-ML Sn/Cu(001).[8,13,14]

II. EXPERIMENT

Experiments using ARPES and LEED were performed in an ultrahigh-vacuum system with a base pressure lower than

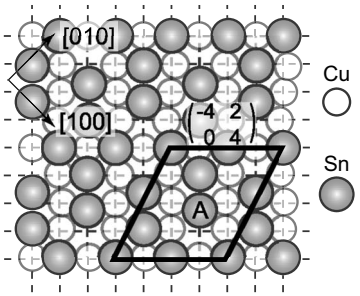

FIG. 1. Schematic model of the surface structure. Gray and white circles denote Sn and Cu atoms, respectively. Dashed lines show (1×1) lattice of the Cu(001) surface. The parallelogram indicates the unit cell of the surface.

1.0×10^{-10} Torr. Prior to deposition, a Cu(001) single crystal substrate was prepared by several cycles of 1 keV Ar^+ sputtering and subsequent annealing up to 870 K in a few minutes. Orderliness and cleanliness of the surface were checked by a sharp (1×1) LEED pattern and an x-ray photoemission spectroscopy (XPS). Tin was then deposited onto the surface kept at RT from an alumina crucible heated with a tantalum filament at a rate below 0.01 ML/min. At this stage, 1/3-ML, 3/8-ML, and 1/2-ML Sn/Cu(001) domains coexist on the surface even if the deposition rate is carefully controlled as reported in the previous STM and LEED observations.[21] Thus, in the present study, the surface after the Sn deposition was annealed at 405 K for five minutes to prepare a well-ordered wide terrace of 3/8-ML Sn/Cu(001).

In the ARPES measurements, we used an angular mode of a hemispherical electron energy analyzer (VG SCIENTA SES100) with unpolarized He II ($h\nu$=40.82 eV) radiation as a photon source. The sample temperature during the ARPES measurement was set to 425 K (HT), 360 K (MT), RT, and 125 K (LT). The LEED patterns were observed in the same temperature range. The surface structure was observed using STM (Omicron, Micro-STM) in another ultrahigh-vacuum chamber at RT. All the measurements were finished in 48 h after the Sn deposition. After the measurement, surface contamination was checked by means of LEED and XPS. For the temperature dependence of the LEED pattern, the patterns were observed in the same temperature range within 3 h after the surface was made. In addition, we confirmed that high-resolution STM images can be taken in 72 h after the Sn deposition.

Energy band dispersion for the wave vector parallel to the surface ($k_\parallel$) can be obtained from the ARPES spectra using the following formula: $k_\parallel=0.512\sqrt{(h\nu-E_B-E_W)}$, where E_B is a binding energy and E_W is a work function of the sample. The work function was experimentally determined from the cut-off energy of secondary photoelectrons.

III. RESULTS AND DISCUSSION

A. Structure

First, we summarize the structure of 3/8-ML Sn/Cu(001) surface studied by STM at RT.[21] Fig. 1 shows a schematic model of the surface structure. The structure is completely different from those reported for the 1/3-ML and 1/2-ML Sn/Cu(001). The height of the protrusions in the STM image shown in Ref. 21 is the same as that of the Sn atoms on the 1/2-ML Sn/Cu(001). The observed protrusions on the surface was thus identified as Sn atoms embedded into the first layer of Cu substrate as on the 1/2-ML Sn/Cu(001) surface. In the model, we arbitrarily extract some of the surface Cu atoms to make the Sn position consistent with the observed STM image. Parallelogram drawn in the figure indicates a unit cell of the structure. A periodicity of this model corresponds to $\begin{pmatrix}-4 & 2\\ 0 & 4\end{pmatrix}$ structure, which agrees with the reported LEED pattern.[20] The Sn atom replacing the Cu atom at the center of the unit cell (labeled A) locates at a position slightly shifted toward $[1\bar{1}0]$ direction. The Sn coverage for this model is 3/8-ML, and is smaller than that estimated only from the deposition rate in the former report.[20] On the other hand, these surface structure and Sn-coverage for 3/8-ML Sn/Cu(001) agree with the results by Lallo *et al.*[22]

We continuously observed the LEED pattern from the 3/8-ML Sn/Cu(001) surface between 125 K and 425 K to study the phase transition. Figs. 2(a) and 2(b) show typical LEED patterns at 125 K and 425 K, respectively. These patterns were taken at primary electron beam energy 125 eV. The $\begin{pmatrix}-4 & 2\\ 0 & 4\end{pmatrix}$ periodicity with two domains has been observed at 125 K, and a (1×1) LEED pattern appears at 425 K. The observed periodicity of the surface in the HT phase is different from the previously observed one, $p(2\times2)$, while the periodicity in the LT phase is the same as the previous one.[20] We will discuss the discrepancy at the end of this subsection.

It is impossible to make a (1×1) ordered structure in the HT phase by moving surface Sn atoms of 3/8-ML coverage in the LT structural model shown in Fig. 1 with the $\begin{pmatrix}-4 & 2\\ 0 & 4\end{pmatrix}$ periodicity. We consider that the mono-layer Sn coverage must be needed for making a (1×1) ordered structure at HT phase. This obviously contradicts the density of the Sn atoms at the surface. Thus, the most plausible transition is that between the low-temperature ordered structure and high-temperature thermally-disordered one without a long-range order. The observed (1×1) LEED pattern in the HT phase should originate from the Cu(001)-(1×1) substrate.

Fig. 3(a) shows observed temperature dependence of the LEED-spot intensity (*I-T*). The raw data of the (3/4 0) spot intensity, which is attributed to the ordered structure of 3/8-ML Sn/Cu(001), are given as solid circles in the figure. The intensity gradually decreases with increasing temperature, drastically reduces above 360 K, and finally disappears around 385 K. Note that the intensity below 385 K is continuously varied. We confirmed that the intensity change is reversible without hysteresis within our experimental accuracy. This behavior allows us to interpret the phase transition as second-order transition.

We corrected the Debye-Waller factor in the raw *I-T* data to discuss the critical exponent of the phase transition. Here, we used the low-temperature (280–330 K) part of the data by fitting them to a decaying exponential function to obtain the curve for the correction. The corrected *I-T* data are shown in Fig. 3(a) as open circles.

We analyzed the corrected *I-T* curve derived from the (3/4 0) diffraction intensity using a power law function, $I(T)$

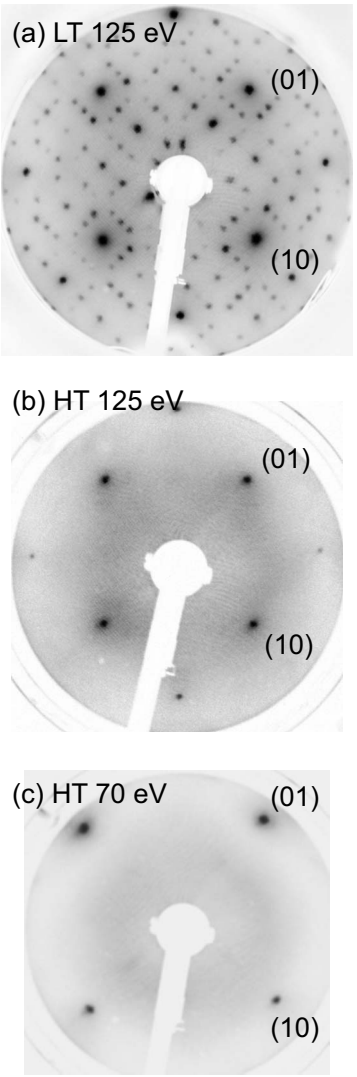

FIG. 2. LEED patterns from the 3/8-ML Sn/Cu(001) surface at the HT (425 K) and LT (125 K) phases. The primary electron energy was set to (a) and (b) 125 eV and (c) 70 eV.

$\propto (1-T/T_C)^{2\beta}$. Here, β is a critical exponent, and T_C is an *order-disorder* transition temperature.[23,24] It is noted that the power law is applicable to the *I-T* curve only in the vicinity of T_C of the second-order phase transition. Thus, we used the following process in the analysis. First, the T_C was estimated to be 381 ± 1 K as the inflection point on the *I-T* curve, which was determined by taking its derivative. Next, the logarithmic intensity versus the logarithmic $(1-T/T_C)$ below the transition temperature was plotted as in Fig. 3(b). In the fitting procedure, we used the data only between 335 and 381 K, just below the critical temperature. The critical exponent β was fixed to be $\beta=0.13\pm0.02$ as a slope of the logarithmic plot. The obtained *I-T* curve shown by dashed line in Fig. 3(a) reproduces the experimental result well. We also analyzed the LEED intensity of the (3/4 1/8) diffraction spot, which is also attributed to the ordered structure of 3/8-ML Sn/Cu(001). The obtained T_C and critical exponent β agree with the above values within the error. The β value supports that the 3/8-ML Sn/Cu(001) surface shows the second-order transition. The transition temperature thus obtained is

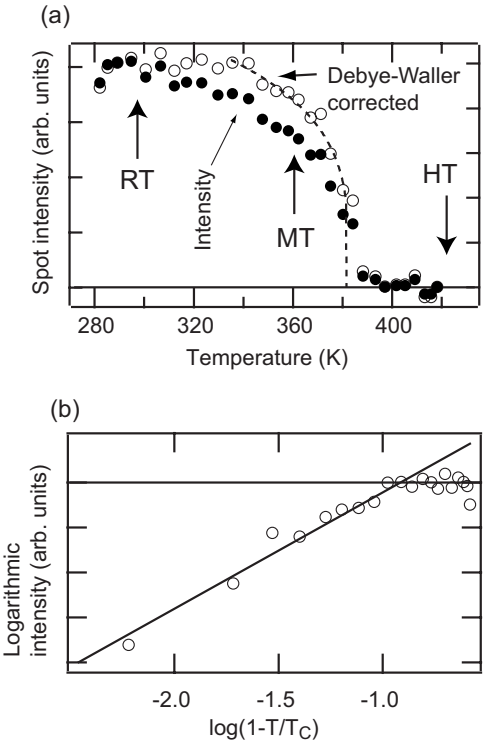

FIG. 3. (a) Solid and open circles show the LEED intensities of the (3/4 0) spots for the 3/8-ML Sn/Cu(001) surface as a function of temperature without and with the Debye-Waller correction, respectively. Dashed line indicates the curve fitted to a power law function; $I(T) \propto (1-T/T_C)^{2\beta}$ with $T_C=381$ K and $\beta=0.13$. (b) Logarithmic intensity versus logarithmic $(1-T/T_C)$ below the transition temperature. Solid lines indicate the fitted line with the power law.

slightly higher than that of 1/2-ML Sn/Cu(001), in which the LT $(3\sqrt{2}\times\sqrt{2})R45°$ phase reversibly changes to the HT $(\sqrt{2}\times\sqrt{2})R45°$ phase at ~360 K.[8]

For *order-disorder* transitions, values of critical exponent β are 1/8, 1/9, and 1/12 for the two-dimensional Ising, 3-states and 4-states Potts universality classes, respectively.[25] The observed *order-disorder* transition of 3/8-ML Sn/Cu(001) surface may fall into the universality class of the two-dimensional Ising or 3-states Potts models. For 0.63-ML In-adsorbed Cu(001) surface, which also shows *order-disorder* transition between the LT $c(4\times4)$ phase and the HT $p(2\times2)$ phase at 345 K, the critical exponent β was estimated to be 0.15 ± 0.19.[9] The β for 3/8-ML Sn/Cu(001) roughly agrees with the β for 0.63-ML In/Cu(001).

In the last of this subsection, we briefly discuss the discrepancy of the periodicity in the HT phase between the present work (1×1) and the previous result $p(2\times2)$ reported in Ref. 20. In our LEED study, the (1×1) LEED pattern was always observed in the HT phase when the primary beam energy was fixed between 40 and 200 eV, even at the same energy in Ref. 20. For example, we show the result at 70 eV in Fig. 2(c). Thus, the discrepancy is not caused by the difference of the beam energy.

Any ordered (2×2) or (2×1) periodicity cannot be made on the 3/8-ML Sn/Cu(001) surface because of the inconsistency of the density of the Sn atoms on the surface as discussed for the (1×1) structure. Note that the single domain

of the LT phase does not yield the (1/2 1/2) LEED spots. The observed (1/2 1/2) and (1/2 0) spots in the LEED pattern of the LT phase originate from the 2×4 periodicity with two domains. Thus, the (1/2 1/2) spots could appear from the 2×4 periodicity with two domains at a high temperature if the periodicity of the LT phase remains only in the Sn atoms located at the (2×4) positions and the other Sn atoms are disordered. This structure is, however, not an ordered surface structure.

Experimentally, we point out the difference in the Sn coverage on the surface between the present study and that in Ref. 20. In our study, the coverage is 3/8 ML, which was determined by the STM observation and is consistent with the estimation by the deposition rate. Whereas in the reported study in Ref. 20, the Sn coverage for 3/8-ML Sn/Cu(001) was assigned 0.45-ML by the deposition rate.[20] In the STM study for more than 0.4-ML Sn coverage, we confirmed that the surface consists of both 3/8-ML and 1/2-ML Sn/Cu(001) domains.[21] For the 0.45-ML surface over 360 K, the c(2 $\times$2) LEED pattern from the HT phases of the 1/2-ML Sn/Cu(001) domains should be mixed with the (1×1) pattern. The (1/2 1/2) spots reported in the Ref. 20 can be interpreted as those from the HT phase of 1/2-ML Sn/Cu(001). However, the existence of (1/2 0) spots cannot be explained by the simple mixture model of the 3/8-ML and 1/2-ML Sn/Cu(001) domains.

B. Electronic state

The electronic structure of 3/8-ML Sn/Cu(001) was investigated by ARPES. We rotated the polar (θ) and azimuthal angles (ϕ) of the sample. Fig. 4(a) shows SBZ's for 3/8-ML Sn/Cu(001). Here, [100] direction ($\bar{\Gamma}\bar{M}$ direction) is defined as the azimuthal angle $\phi=0°$. The gray line denotes the SBZ for the 1×1 HT phase. The SBZ's for two domains of the LT phase with the $\begin{pmatrix}-4 & 2\\ 0 & 4\end{pmatrix}$ periodicity are shown as thin gray (green) and dashed (blue) lines.

Figs. 4(b) and 4(c) show the ARPES results of 3/8-ML Sn/Cu(001) for the HT and LT phases, respectively. These were taken on the line (l) ($\phi=0°$) in $\bar{\Gamma}\bar{M}$ direction of SBZ shown in Fig. 4(a). A dispersive band as marked with triangle symbols, which crosses E_F, is seen in the HT phase. The dispersion agrees with the *free-electron-like* behavior. On the other hand, the band folds back at LT. It is noted that the bands due to Cu 3*d* states were excited by coexisting He II$_\beta$ radiation and detected in the spectra as marked with short line symbols.

The energy band dispersion (2nd derivative) images and the energy distribution curves (EDC's) of the spectral intensity measured at HT, 360 K (MT), RT, and LT are drawn in left and right panels in Figs. 5(a)–5(d), respectively. At MT, the intensity of the $\begin{pmatrix}-4 & 2\\ 0 & 4\end{pmatrix}$ LEED spots are ~40% reduced [see Fig. 3(a)]. In the HT phase, a dispersive band crossing E_F was detected as shown in Fig. 5(a). For 1/2-ML Sn/Cu(001), a similar band crossing the Fermi level is known and identified as an *sp-like* surface resonance band.[8,11,13] Here, we also call this band for 3/8-ML Sn/Cu(001) S band as in 1/2–ML one. The Sn-induced *sp-like* surface resonance bands in the same direction also appear for the clean

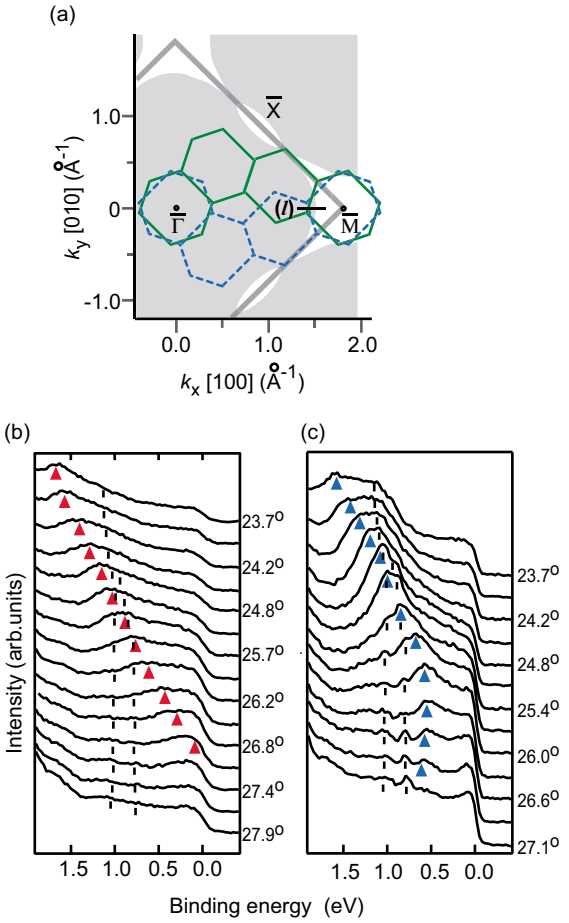

FIG. 4. (Color online) (a) Surface Brillouin zones (SBZ's). Thick gray line denotes (1×1). Thin gray (green) and dashed (blue) lines show the SBZ's of 3/8-ML Sn/Cu(001), where the lines represent two different domains. Unshaded areas denote bulk band gaps. Line (l) corresponds to the range of the measurement with azimuthal angle $\phi=0°$. (b), (c) ARPES spectra ($h\nu=40.82$ eV) for 3/8-ML Sn/Cu(001) at 425 K (HT phase) and at 125 K (LT phase), respectively. The ARPES spectra were taken along line (l) shown in Fig. 4(b). Triangle symbols denote the Sn-induced surface resonance bands. Short line symbols are attributed to Cu 3*d* states excited by He II$_\beta$ radiation.

Cu(001), 1/5-ML, and 1/3-ML Sn/Cu(001) surfaces,[14] and slightly depend on the surface structure. This is because the wave function of the S band penetrates into the bulk.[11] Consequently, the S band can appear for the disordered surface in the HT phase.

The dispersion of the S band continuously changes with decreasing temperature from the HT to LT phases as in Figs. 5(a)–5(d). Triangles in the EDC spectra show the peak positions which are marked on the basis of the 2nd derivative images. The bands observed at RT and LT fold back with an energy gap 0.41 eV and 0.50 eV below E_F, respectively. Here, the gap energy was estimated from the peak position of EDC's. The backfolding band originates from the ordered area with the $\begin{pmatrix}-4 & 2\\ 0 & 4\end{pmatrix}$ periodicity. At MT, two component dispersions can be recognized as indicated by the dark area of the 2nd derivative images and the triangles in Fig. 5. The dispersion crossing E_F agrees with that in the HT phase

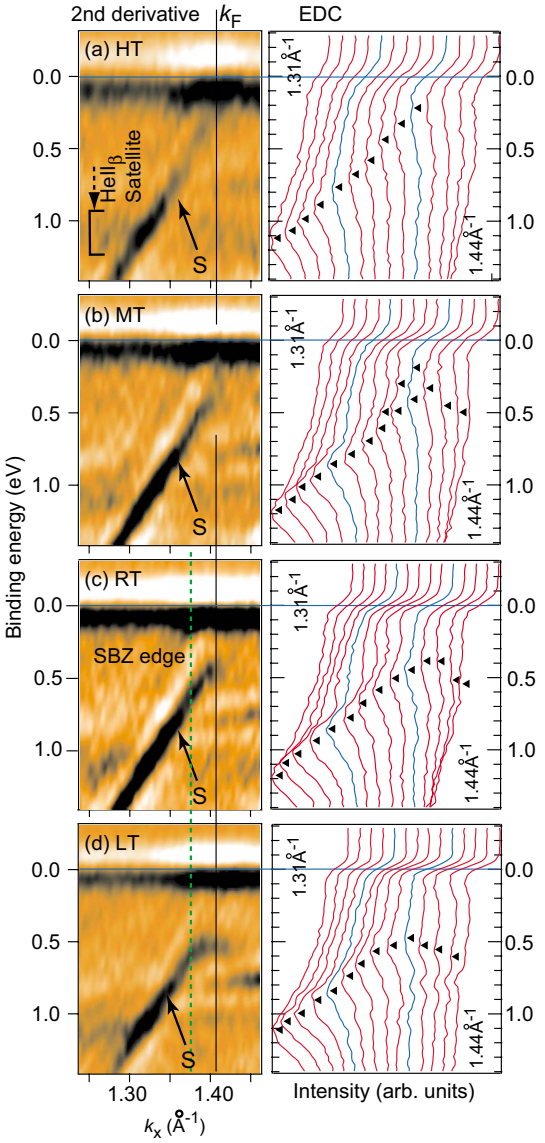

FIG. 5. (Color online) (a)-(d) Experimental energy band dispersions (2nd derivative) and the energy distribution curves (EDC's) of the spectral intensity for 3/8-ML Sn/Cu(001) at 425 K (HT), 360 K (MT), RT, and 125 K (LT), respectively, named as S. Bands lying around 1.0 eV are bulk electronic states exited by He II$_\beta$ radiation along the $\bar{\Gamma}\bar{M}$ symmetry direction of the SBZ. Vertical dashed line (black) in (a) represents the position of the Fermi wave number k_F of S band. Vertical bold dashed line (green) shows the position of the SBZ boundary for the LT phase. Triangle symbols in the right panels denote the S bands.

shown in (a). Another one folds back at the vicinity of k_F with the energy gap opening (~0.4 eV) below E_F. The temperature dependence of the band dispersions indicates that the energy gap opens almost at T_C of the structural transition and increases with decreasing the temperature.

We investigated the S band in the HT phase for several selected azimuthal angles (ϕ) with respect to the $\bar{\Gamma}\bar{M}$ direction. The sample temperature was kept at 425 K during the measurements. In Fig. 6(a), the solid lines denote the selected ϕ's. The dispersions of the S band in the HT phase on these lines are exhibited in Fig. 6(b). The S bands measured at ϕ=6 and 12° cross E_F while the band at ϕ=22° has an energy gap. This behavior is similar to the band structure reported for the In/Cu(001) surface alloy.[10] In Fig. 6(b), a Cu bulk band was also observed, and the intensity of its signal increases with approaching to $\bar{\Gamma}\bar{X}$ symmetry axis.[10,26]

The Fermi surface of the S band for 3/8-ML Sn/Cu(001) in the HT phase can be drawn using the obtained values of k_F. In Fig. 6(a), k_F at each ϕ is marked as a solid circle, and a possible Fermi surface of the S band is shown as a solid curve. Here, it is assumed that the shape of the Fermi surface has a *free–electron-like* circle. The estimated radius is ~1.38 Å^{-1} and smaller than that of the 1/2-ML Sn/Cu(001).[8,13]

We measured the dispersions of the S band for the LT phase at several ϕ's. The S band in the LT phase always folds back in the vicinity of k_F for the HT phase as shown in Figs. 6(c) for ϕ=3,6,11°. The observed energy gap below E_F is commonly ~0.5 eV. The experimental results clearly indicate that the electronic state of the 3/8–ML Sn/Cu(001) surface significantly changes with the *order-disorder* transition.

In the images of the dispersions, vertical solid lines denote the positions of k_F of the S band in the HT phase, and vertical bold dashed lines (green and blue) represent the positions of the SBZ edge for the $\begin{pmatrix} -4 & 2 \\ 0 & 4 \end{pmatrix}$ phase. The band can fold back at the SBZ edge. It is noted that there are several SBZ edges in the measured regions for ϕ=3 and 6° because of the existence of the two domains in the LT phase. For ϕ=11°, the SBZ edges are not included in the measured range. In the case of ϕ=3°, there are three SBZ edges in the observed k space. One of them is close to k_F for the HT phase and the other two edges are located at lower and higher wave number sides compared with k_F, respectively. Here, k_F for ϕ=3°, which corresponds to ~1.38 Å^{-1}, is extrapolated from the circular Fermi surface as shown in Fig. 6(a). Consequently, it is difficult to fix whether the S band folds back at k_F for the HT phase or the SBZ edge. On the other hand, in the cases of ϕ=6° and 11°, the S band folds back in the vicinity of k_F while the SBZ edges of the LT phase are considerably away from k_F at ϕ=6 and 11°.

As mentioned in Sec. I, the energy gap appears in the S band of 1/2-ML Sn/Cu(001) only at the SBZ edge of the LT $3\sqrt{2}$ phase. It diminishes when the k vector leaves from the $\bar{\Gamma}\bar{M}$ direction.[8,13,14] This is quite in contrast to the present results in 3/8-ML Sn/Cu(001). Below T_C, the S band of 3/8-ML Sn/Cu(001) always folds back in the vicinity of k_F for the HT phase irrespective of the position of the SBZ edges. In addition, the amplitude of the energy gap for the band at each ϕ is roughly the same. We consider that the electronic energy plays an important role in the structural transition because the structural transition occurs to minimize the total free energy of the system including both lattice and electrons. The energy gap formation of the S band decreases the electronic energy, and favors the structural transition. At present, however, there is no explanation for the gap formation at the points far from the SBZ edge in *k space* for the *order-disorder* transition. The exiting CDW scenarios are inconsistent with the observed results as described in the following subsection. The surface lattice and electronic

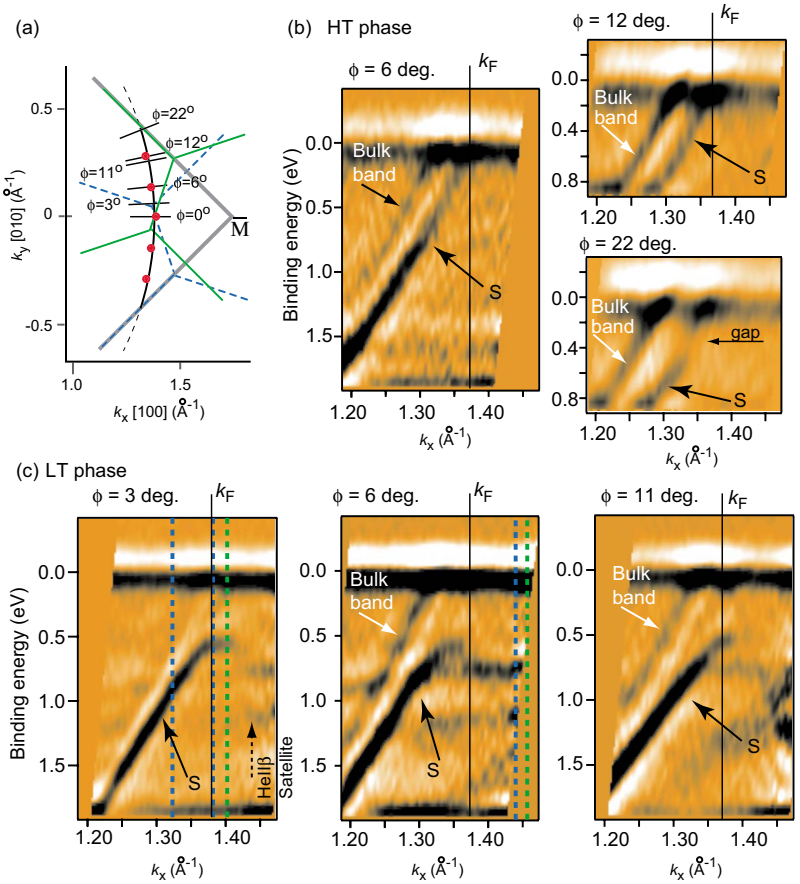

FIG. 6. (Color online) (a) Magnified SBZ focusing around the $\overline{M}$ symmetry point. Thick gray lines show the SBZ for the 1×1 surface. Thin gray (green) and dashed (blue) lines denote the SBZ of 3/8-ML Sn/Cu(001) with two domains in the LT phase. Circular symbols indicate the positions of k_F for S bands obtained from the ARPES measurement with selected azimuthal angles (ϕ) in the HT phase. Extrapolated Fermi surface of the S bands is drawn by solid curve. (b) Electronic band dispersions (2nd derivative) for 3/8-ML Sn/Cu(001) at 425 K (HT phase) for the selected ϕ's. Solid lines denote the positions of k_F. (c) Dispersions of the surface resonance bands at 125 K (LT phase) for the selected ϕ's. Gray dashed (blue and green dashed) lines are guides for eye on the SBZ edges of LT phase.

structures should be investigated in detail to clarify the origin of the gap formation.

C. Comparison with CDW scenario

In the last subsection, we compare the observed structural transition for the 3/8-ML Sn/Cu(001) surface with the CDW scenario as in Ref. 14. The CDW nature is classified into three categories, i.e., the weak coupling CDW with long coherence, the strong-coupling CDW with short or long coherence.[11]

One of the important features for the weak-coupling CDW mechanism is Fermi surface nesting due to weak electron-phonon coupling. As shown in Fig. 4, in $\overline{\Gamma}\overline{M}$ direction, the S band folds back at k_F for the HT phase, which is the vicinity of the SBZ edge at LT phase. However, for $\phi=3,6,11°$ in Fig. 6, the folding back points are away from the SBZ edges for LT phase. These indicate that the nesting condition is satisfied only at a small fraction around $\overline{\Gamma}\overline{M}$ direction. It is, therefore, considered that the gain of energy by the Fermi surface nesting is not sufficient for the structural phase transition. In addition, the gap energy below Fermi level is ~0.5 eV at LT phase. In the theory of weak-coupling CDW, the gap energy Δ is described by the formula $\Delta=1.76k_BT_C$.[27,28] However, the observed value of Δ is much larger than that estimated from the observed T_C using this formula. Thus, the weak-coupling CDW is inconsistent with the observed results.

A narrow area of the 3/8-ML Sn/Cu(001) structure in 1/2-ML Sn/Cu structure was previously reported in Ref. 21. Fig. 7 exhibits an STM image with a very small 3/8-ML Sn/Cu(001) domain ($\sim2.5\times1.5$ nm^2), named A, surrounded by a disordered area. The observed protrusions on the surface can be identified as Sn atoms embedded into the first layer of Cu substrate. The parallelogram denotes the unit cell of the $\begin{pmatrix}-4 & 2\\ 0 & 4\end{pmatrix}$ structure. Only $1\sim2$ periodic structures of 3/8-ML Sn/Cu(001) phase exist within the area A. If the $\begin{pmatrix}-4 & 2\\ 0 & 4\end{pmatrix}$ structure is due to the CDW, this result indicates its correlation length (ξ) to be as short as $1.5\sim2.5$ nm. Thus, the observed narrow structure disagrees with both the weak-coupling and strong-coupling CDWs with a long correlation length.

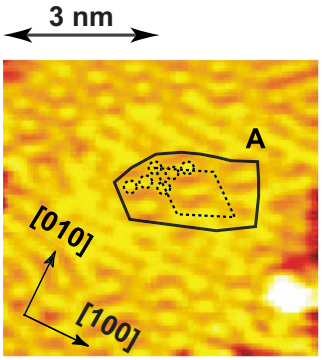

FIG. 7. (Color online) STM image of coexisting surface of 3/8-ML and disordered Sn/Cu(001) areas. Parallelogram in the domain A denote the unit cell of 3/8-ML Sn/Cu(001).

The strong-coupling CDW with short coherence cannot explain the observed gap extending δk in the k space (~ 0.1 Å^{-1}) and the gap energy (0.5 eV), which are evaluated from the S band shape for LT phase shown in Fig. 5. The gap extending ~ 0.1 Å^{-1} means that the CDW correlation length should be longer than ~ 6 nm by $2\pi/\xi$. This value is longer than the observed domain size. In other words, if the 3/8-ML Sn/Cu(001) phase is interpreted as the strong-coupling CDW with a short correlation length as short as ~ 2 nm, the gap extending in reciprocal space and the top of the S band should be more than 0.3 Å^{-1} and 2 eV below E_F, respectively. Furthermore, the band gap opens at almost the same temperature of the structural phase transition, which also disagrees with the feature of the strong-coupling CDW with short coherence. Thus, the phase transition cannot be interpreted by any type of the existing CDW models.

IV. CONCLUSION

The structural and electronic properties have been studied using STM, LEED, and ARPES for 3/8-ML Sn/Cu(001) surface. It is shown by the LEED observations that the surface shows a temperature induced reversible structural transition between $\begin{pmatrix} -4 & 2 \\ 0 & 4 \end{pmatrix}$ periodicity in the LT phase and (1×1) periodicity in the HT phase. We have interpreted the structural transition as an *order-disorder* transition on the basis of the structure model. The transition temperature and the critical exponent β was estimated from temperature dependence of LEED intensity analysis. The Sn-induced surface resonance band of 3/8-ML Sn/Cu(001) in the HT and LT phases was measured by means of the ARPES. The energy band dispersion agrees with the free-electron character in the HT phase. For the LT phase, the band folds back with an energy gap. The folding points of the band at the selected ϕ's are close to k_F in reciprocal space of the HT phase, and are independent of the SBZ edges. In addition, the amplitudes of the energy gap at the ϕ's are roughly the same. The electronic states of the 3/8-ML Sn/Cu(001) surface significantly change with the *order-disorder* transition. The phase transition cannot be explained by the existing CDW models. It is necessary to develop a new concept for understanding the present results on the phase transition of 3/8-ML Sn/Cu(001) surface.

ACKNOWLEDGMENTS

STM images were analyzed with a program code (easy-SPM) developed by K. Tomatsu. The authors are also grateful to M. Yamada for fruitful discussion.

*Department of Chemistry, Graduate School of Science, Kyoto University, Kyoto 606–8502, JAPAN; yaji@kuchem.kyoto-u.ac.jp
†komori@issp.u-tokyo.ac.jp

[1] C. Binns, and C. Norris, J. Phys.: Condens. Matter **3**, 5425 (1991).
[2] T. Nakagawa, G. I. Boishin, H. Fujioka, H. W. Yeom, I. Matsuda, N. Takagi, M. Nishijima, and T. Aruga, Phys. Rev. Lett. **86**, 854 (2001).
[3] X. Gao, Y. M. Zhou, S. C. Wu, and D. S. Wang, Phys. Rev. B **66**, 073405 (2002).
[4] T. Nakagawa, S. Mitsushima, H. Okuyama, M. Nishijima, and T. Aruga, Phys. Rev. B **66**, 085402 (2002).
[5] T. Aruga, J. Phys.: Condens. Matter **14**, 8393 (2002).
[6] T. Nakagawa, H. Okuyama, M. Nishijima, T. Aruga, H. W. Yeom, E. Rotenberg, B. Krenzer, and S. D. Kevan, Phys. Rev. B **67**, 241401(R) (2003).
[7] S. Hatta, H. Okuyama, M. Nishijima, and T. Aruga, Phys. Rev. B **71**, 041401(R) (2005).
[8] J. Martínez-Blanco, V. Joco, H. Ascolani, A. Tejeda, C. Quirós, G. Panaccione, T. Balasubramanian, P. Segovia, and E. G. Michel, Phys. Rev. B **72**, 041401(R) (2005).
[9] S. Hatta, H. Okuyama, T. Aruga, and O. Sakata, Phys. Rev. B **72**, 081406(R) (2005).
[10] T. Nakagawa, H. W. Yeom, E. Rotenberg, B. Krenzer, S. D. Kevan, H. Okuyama, M. Nishijima, and T. Aruga, Phys. Rev. B **73**, 075407 (2006).
[11] T. Aruga, Surf. Sci. Rep. **61**, 283 (2006).
[12] V. Joco, J. Martínez-Blanco, P. Segovia, T. Balasubramanian, J. Fujii, and E. G. Michel, Surf. Sci. **600**, 3851 (2006).
[13] J. Martínez-Blanco, V. Joco, J. Fujii, P. Segovia, and E. G. Michel, Phys. Rev. B **77**, 195418 (2008).
[14] K. Yaji, Y. Nara, K. Nakatsuji, T. Iimori, K. Yagyu, R. Nakayama, N. Nemoto, and F. Komori, Phys. Rev. B **78**, 035427 (2008).
[15] C. Argile and G. E. Rhead, Thin Solid Films **87**, 265 (1982).
[16] C. Argile and G. E. Rhead, Surf. Sci. **135**, 18 (1983).
[17] E. McLoughlin, A. A. Cafolla, E. AlShamaileh, and C. J. Barnes, Surf. Sci. **482-485**, 1431 (2001).
[18] A. A. Cafolla, E. McLoughlin, E. AlShamaileh, Ph. Guaino, G. Sheerin, D. Carty, T. McEvoy, C. Barnes, V. Dhanak, and A. Santoni, Surf. Sci. **544**, 121 (2003).
[19] K. Pussi, E. AlShamaileh, E. McLoughlin, A. A. Cafolla, and M. Lindroos, Surf. Sci. **549**, 24 (2004).
[20] J. Martínez-Blanco, V. Joco, P. Segovia, T. Balasubramanian, and E. G. Michel, Appl. Surf. Sci. **252**, 5331 (2006).
[21] Y. Nara, K. Yaji, T. Iimori, K. Nakatsuji, and F. Komori, Surf. Sci. **601**, 5170 (2007).
[22] J. Lallo, L. V. Goncharova, B. J. Hinch, S. Rangan, R. A. Bartynski, and D. R. Strongin, Surf. Sci. **602**, 2348 (2008).
[23] Z. Li, X. Liang, M. L. Stutzman, J. A. Spizuoco, S. Chandavarkar, and R. D. Diehl, Surf. Sci. **327**, 121 (1995).
[24] M. Schick, Prog. Surf. Sci. **11**, 245 (1981).
[25] F. Y. Wu, Rev. Mod. Phys. **54**, 235 (1982).
[26] C. Baldacchini, L. Chiodo, F. Allegretti, C. Mariani, M. G. Betti, P. Monachesi, and R. Del Sole, Phys. Rev. B **68**, 195109 (2003).
[27] R. E. Peierls, *Quantum Theory of Solids* (Clarendon, Oxford, 1955).
[28] H. Fröhlich, Proc. R. Soc. London, Ser. A **233**, 296 (1954).